Food Chemistry: X 26 (2025) 102337

Contents lists available at ScienceDirect

Food Chemistry: X

journal homepage: www.sciencedirect.com/journal/food-chemistry-x

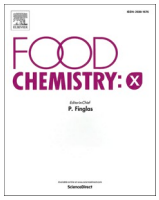

Sweet-enhancing effect of coolant agent menthol evaluated via sensory analysis and molecular modeling

Haiyan Yu [a], Ting Ao [a], Haifang Mao [b], Jibo Liu [b], Chen Chen [a], Huaixiang Tian [a,*]

[a] Department of Food Science and Technology, Shanghai Institute of Technology, Shanghai 201418, China
[b] School of Chemical and Environmental Engineering, Shanghai Institute of Technology, Shanghai 201418, China

ARTICLE INFO

Keywords:
Cross-modal interaction
Sugar reduction
Menthol
High-fructose corn syrup
Molecular docking
Molecular dynamics simulation

ABSTRACT

Responding to global trends favoring low-sugar diets, this study explored the potential of menthol, a cooling agent, to enhance sweet taste perception through integrated sensory evaluations and molecular modeling. The results of static sensory evaluation (recognition threshold determination, paired comparison test and 15 cm-linear scale) and dynamic sensory analysis indicated that menthol lowered sweetness threshold of HFCS (from 5.98 g/L to 5.02 g/L), while intensifying maximum sweetness intensity and prolonging the duration of sweetness. Sensory analysis identified optimal sweet enhancement at 0.004–0.030 g/L menthol concentrations, while 0.060 g/L caused sweetness suppression through intensified cooling/bitter sensations. Molecular modeling comparing T1R2/T1R3-Glu/Fru system and T1R2/T1R3-Glu/Fru/Men system elucidated that the addition of menthol increased the number of hotspot residues in protein-sugars binding and stabilized interactions by occupying sites near sugar active sites, maintaining the Venus Flytrap Domain in its closed, activated configuration. These findings demonstrated the underlying contribution menthol made to sweet enhancement and sugar reduction.

1. Introduction

The World Health Organization has recommended free sugar intake to be less than 10 % of total daily energy, a further reduction to <5 % of total daily energy is encouraged for added health benefit (WHO, 2015). The consumption of sugar-sweetened beverage, a widespread dietary habit among urban youth, has become one of the leading sources of excessive free sugars intake (Miele et al., 2017). The free sugars in beverages are mainly sucrose and high-fructose corn syrup (HFCS). The excessive consumption of added sugars results in adverse health outcomes. Consequently, many countries and regions with high sugar-sweetened beverages (SSB) consumption levels have introduced intervention policies, such as SSBs consumption tax, to reduce consumers' sugar consumption levels (Zhai et al., 2024). The trend towards sugar-free and low-sugar beverages is gaining momentum globally (Chen et al., 2022; Deliza et al., 2021). The approaches to low-sugar beverages revolves around sugar reduction and artificial sweeteners. Given consumers' reluctance to compromise on taste, current research endeavors are directed towards the innovation of novel, high-intensity, low-additive non-nutritive sweeteners. These sweeteners may not fully replicate the taste and effectiveness of traditional nutritive sweeteners (Miele et al., 2017) and their safety remains a subject of controversy (Maluly et al., 2020). Increasingly, consumers are adopting long-term low-sugar dietary practices to reduce the stimulatory effect of sweetness and enhance their sensitivity to sweetness (da Portela et al., 2024). Nevertheless, due to inherent biological constraints, dietary habits, and environmental influences, implementing such practices can be challenging and require sustained effort over a prolonged period. Therefore, there is an urgent need to explore sugar reduction methods that offer consumers a pleasant sensory experience.

The interplay of cross-modal perception refers to the stimulation of one sense (e.g., olfaction) that satisfies or enhances the experience of another sense (e.g., gustation) (Biswas & Szocs, 2019). Study have demonstrated that specific odors can amplified taste perception intensity (Ai & Han, 2022). Additionally, there are evidences that chemesthesis, the perception of chemical stimuli distinct from taste and smell, interacts with basic taste modalities (Sun et al., 2023; Wang et al., 2022). Steven Pringle noted that cool-sensing ingredients, such as menthol, have potential applications in enhancing flavor perception (McDonald et al., 2016). Therefore, it is hypothesized that leveraging chemesthesis, particularly through agents like menthol, could achieve a synergistic enhancement of sweetness perception. Cooling agents (e.g., menthol) elicit a cooling sensation by directly stimulating chemically

* Corresponding author.
E-mail address: tianhx@sit.edu.cn (H. Tian).

https://doi.org/10.1016/j.fochx.2025.102337
Received 10 January 2025; Received in revised form 18 February 2025; Accepted 26 February 2025
Available online 28 February 2025

Nomenclature

STR	sweet taste receptors
HFCS	high-fructose corn syrup
VFD	venus flytrap domain
GPCRs	C G protein-coupled receptors
PDB	protein data bank
RSD	relative standard deviation
MD	molecular dynamic
PME	Particle-mesh Ewald
TMD	transmembrane domain
CRD	cysteine-rich domain
RMSD	root mean square deviation
RMSF	root mean square fluctuation
Rg	radius of Gyration
SASA	solvent-accessible surface area
AUC	area under the curve
SATI	single-attribute time-intensity
MATI	multi-attribute time-intensity

sensitive fibers, which are part of the nociceptive and temperature-sensitive fiber network (McDonald et al., 2016). Current research on cooling sensation primarily focuses on its underlying mechanisms (Xu et al., 2020), with limited exploration into the interaction between cooling sensation and taste perception.

Currently, the exploration of cross-modal sensory interaction mechanisms primarily relies on artificial sensory evaluation. This approach serves dual purposes: to discover and characterize substances that enhance or suppress flavors, as well as to assess the sensory effects of these compounds (Büchner et al., 2022; Rocha et al., 2020). Artificial sensory evaluation encompasses both static and dynamic sensory analyses. Static sensory analysis aims to provide a comprehensive assessment of a product's sensory attributes, whereas dynamic sensory analysis focuses on the changes in specific sensory characteristics over time (Vidal et al., 2019). In addition to sensory analysis, multidisciplinary techniques and methodologies, such as molecular modeling, are being harnessed. Molecular modeling is gradually gaining traction in elucidating the mechanisms underlying sensory responses. It is well-established that human sweet taste receptors (STR) belong to the class C G protein-coupled receptors (GPCRs), consisting of a heterodimer protein formed by the hT1R2 and hT1R3 subunits. Despite the absence of a crystal structure for the human T1R1/T1R3 receptor, Yuan et al. (2024) have employed homology modeling to construct its three-dimensional structure. Prior researches have investigated the interaction mechanisms between various sweet substances and the T1R2/T1R3 receptor protein using molecular docking (Kim et al., 2017; Zhu et al., 2024). Zhang and colleagues further explored the sweetening mechanism of flavor enhancers using molecular docking techniques (Zhang et al., 2010). It is noteworthy that molecular docking may produce false-positive results. Molecular dynamics simulations, however, can not only analyze and validate the binding stability between ligands and receptors but also effectively reduce the false-positive outcomes of molecular docking (Zhao et al., 2024).

Cooling agents are widely employed in food and beverage products-including confectionery, chewing gum, chocolate, ice cream, yogurt, tea, coffee, and carbonated beverages-to enhance sensory attributes such as flavor complexity, palatability, and hedonic appeal, aligning with robust consumer preference. Building upon the premise of favorable consumer acceptance of cooling additives in food and the hypothesis of cross-modal sensory interactions between cooling and sweetness perception, this study evaluates the cross-modal interaction between cooling and sweetness perception, investigating both threshold/suprathreshold responses and underlying molecular mechanisms. Sensory evaluations were conducted to analyze the impact of various menthol concentrations on the sweetness threshold, intensity, and duration of HFCS. Molecular docking was employed to explore the effects of menthol incorporation on binding sites and interaction forces between the STR and ligand molecules. Molecular dynamics simulations were conducted to investigate the dynamic interactions between STR and ligand molecules, thereby assessing the stability of system binding. This research has deepened our understanding of the role of coolness in enhancing sweetness and has provided insights into sugar reduction strategies for the development of low-sugar foods, particularly beverages.

2. Materials and methods

2.1. Reagents

Food grade ethanol (95 %) (Gengma Hualin Alcohol Co., Ltd., Lincang, China); Food grade menthol (Anhui Province Yifan Spice Co., Ltd., Hefei, China); High fructose corn syrup (F55) (Guangzhou Shuangqiao Co., Ltd., Guangzhou, China); Drinking purified water (Hangzhou Wahaha Group Co., Ltd., Hangzhou, China).

2.2. Sample preparation

The test sample concentrations were in weight/volume and are listed in Table S1.

Preparation of sweet sample: Dissolving HFCS in drinking purified water.

Preparation of cooling stock solution: 2.50 g of menthol were accurately weighed and diluted with 95 % ethanol to a final volume of 25 mL, yielding a 100 g/L menthol stock solution.

Preparation of Menthol×HFCS sample: Menthol stock solution was diluted to a specific concentration using purified water, and this diluted menthol solution was then used to prepare the Menthol×HFCS solution.

2.3. Sensory panel and experimental conditions

The study was reviewed and approved by the Ethics Committee of Shanghai Institute of Technology and informed consent was obtained from each subject prior to their participation in the study. The assessors were unaware of the tests' purpose and were compensated after the sensory testing.

The sensory evaluation panel consisted of 30 assessors (10M20F, aged 18–26 years), selected from a group of 60 healthy, non-smoking individuals (32M48F) with prior taste-testing experience. Based on self-reports, all 30 assessors had no oral diseases and no strong preferences or aversions towards food with cooling or sweetness. The assessors' ability to discern the sweetness of HFCS solutions was examined through triangle tests and ranking tests, with accuracy rates exceeding 80 % for triangle tests and 50 % for ranking tests. The selected assessors underwent specialized training to familiarize the evaluation procedures of different sensory experiments and the usage of the APPsense software, along with sensory memory training.

All 30 assessors participated in recognition threshold assessments and paired comparison tests. Additionally, 10 of them (4M6F, aged 21–26) participated in sweetness intensity assessments, including static overall intensity assessments and dynamic time-intensity assessments.

The sensory assessments were conducted in a dedicated sensory assessment room, where the selected assessors worked independently to evaluate the samples in each round of assessment. Solutions samples were prepared fresh daily, and stored in disposable cups at room temperature (25 °C) before sensory evaluation. The sensory evaluation was conducted between 10:00 a.m. and 4:00 p.m. on the day of experiments.

2.4. Test of sweet taste recognition thresholds for HFCS

The sweetness recognition thresholds were determined using a three-alternative forced-choice (3-AFC) ascending concentration series procedure, compliant with ISO 13301:2018 (*Sensory analysis - Methodology - General guidance for measuring odour, flavor and taste detection thresholds by a three-alternative forced-choice (3-AFC) procedure*) (ISO 13301, 2018). The experiment was conducted in 5 trials, each based on five different concentrations of menthol solutions. Each trial comprised 11 rounds of tests, involving two types of solutions: menthol solution without added HFCS (M) as the reference sample, and a mixed solution (MF) with the same menthol concentration as the reference but with added HFCS. Across the 11 samples in each round, the concentration of HFCS increased progressively (concentrations detailed in Table S1A). The two solutions were poured into three cups, with two of the samples being identical, resulting in six possible presentation orders: AAB, ABA, BAA, BBA, BAB, and ABB. and in which the assessor is asked to select the sample perceived as different. If the assessors perceived no difference between the three samples, he or she was instructed to choose one (mandatory choice).

During tasting, assessors were asked to put the sample solution into their mouths, swishing it around to ensure exposure of the entire oral cavity (Johnson et al., 2018). After 5 s, they were to spit out the sample and assess its sweetness. To ensure that the taste and cooling sensation from the previous sample had completely dissipated before evaluating the next sample, assessors were instructed to wait until they could no longer detect any flavor or cooling effect from the previously tasted sample. This was self-assessed by each assessor based on their own sensory perception. Assessors rinsed their mouths with purified water between each sample to further aid in the dissipation process.

The individual threshold of assessor was calculated using the Best Estimate Threshold (BET), where the BET was the geometric mean of the highest concentration at which an incorrect choice was made and the adjacent higher concentration at which a correct choice was made. The individual BETs were then log-transformed, and the panel threshold was determined as the anti-logarithm of the mean of the $\log_{10}$BET. The dispersion of the panel threshold was characterized by the standard deviation of the $\log_{10}$BET. If an assessor makes correct choices for all 11 rounds' concentration levels or makes an incorrect choice at the highest concentration, the concentration gradient should be appropriately expanded, and the testing should continue.

2.5. Establishment of reference scale for sweetness intensity

The sweetness threshold of the HFCS-aqueous solution obtained through thresholds test is 5.98 g/L. Given the application background of beverage production, the sweetness range is moderate, with a sugar content of approximately 40–65 g/L. The initial HFCS concentration was 6.0 g/L, increasing to 68.3 g/L in 1.5-fold steps (concentrations detailed in Table S1B). The establishment of the sweet intensity reference system was based on the reported procedure by (Zhang et al., 2016) with slight modifications, as following steps:

(1) Descriptor Calibration: Assessors first assigned numerical values (0–15 cm scale) to five sweetness intensity descriptors (“slightly sweet”, “a little sweet”, “sweet”, “ relatively sweet” and “very sweet”). The initial scaling ranges for each descriptor were defined by compiling the minimum and maximum values across all assessors. Ambiguities in descriptor overlap were adjusted through subsequent group discussions.
(2) Sensory Evaluation: Assessors then evaluated seven ascending concentrations of HFCS (6.0–68.3 g/L) in triplicate sessions (3-h intervals). For each concentration, they rated perceived sweetness intensity using the adjusted descriptors' scaling range (0–15.0 cm).
(3) Psychophysical Modeling: Stevens' psychophysical laws (expressed as $S = k*I^n$) was applied to model the relationship between HFCS concentration and perceived sweetness intensity. The midpoint concentration of each descriptor's fitted range was selected to anchor the final reference scale.

2.6. Paired comparison test

The paired comparison test was conducted in five trials, each trial consisting of four rounds of testing. In each round, two samples with the same concentration of HFCS were used; one was supplemented with menthol and served as the test sample (M x F), while the other, without menthol, served as the comparison sample (F) (concentrations detailed in Table S1C).

In each group of testing, assessors were required to record the three-number code of the sample that was sweeter between two samples. If the assessors perceived no difference between the two samples, he or she was instructed to choose one (mandatory choice). Two possible presentation orders (AB, BA) were used for each set of test samples, randomly and counterbalanced among sensory panel. The tasting procedure and break between samples adhere to the protocols outlined in Section 2.4.

Rigorous identification criteria were established to ensure the accuracy and reliability of the research. These criteria stipulated that at least half of the panelists must be able to discern differences between the stimulus and control samples, allowing for a high risk at a 95 % confidence level. This translated into a detection probability (Pd) of 50 %, a Type I error probability (α-risk) of 0.05, and a Type II error probability (β-risk) of 0.2. Adhering to the ISO 5495:2005 bilateral testing standard, this assessment determines whether there is a difference in sweetness between the test sample and the control sample by evaluating whether more than 21 out of 30 evaluators make the same choice in each round of testing.

2.7. Overall intensity evaluation of sweetness: 15-cm labeled line scale

10 panelists were instructed to undergo additional training using the established sweetness reference scale, assigning sweetness scores on a scale of 0 to 15 to HFCS solutions with concentrations of 5.98, 9.60, 22.10, 38.10, and 57.20 g/L. This process continued until both individual assessors and the sensory panel achieved a relative standard deviation (RSD) of less than 0.2 for the reference solution scale values. This indicated that the evaluation results of the panel had stabilized, and their reproducibility met the specified requirements (Zhao et al., 2015).

The assessors initially tasted the reference samples (see Table S1C) and memorized their sweetness intensities and corresponding scores. Subsequently, they tasted the test samples, discerned the sweetness intensity of each, and assigned scores using the 15-cm labeled line scale for the sweetness intensity. This process was repeated in three rounds for reproducibility, with a three-hour interval between each round.

2.8. Dynamic sweetness intensity evaluation: Time-intensity test

Dynamic sweetness intensity was evaluated via a time-intensity (TI) test as follows:

(1) Panelist Training: 10 assessors underwent additional training using the established sweetness reference scale. They completed a pre-experiment with three randomly selected reference samples (Table S1C) to familiarize themselves with the TI protocol. Training was conducted using sensory testing software Appsense V10.1.2 (Beijing Yinghuali Technology Co., Ltd., Beijing, China), which automatically recorded sweetness intensity at predefined intervals: every 5 s (0–10 s), 10 s (10–60 s), 15 s (60–180 s), and 30 s (180–300 s). Training concluded when assessors achieved reproducibility criteria: relative standard deviation (RSD) <0.2

for maximum sweetness intensity and RSD <0.4 for the timing of maximum intensity occurrence.

(2) Formal TI Testing: Following ASTM 1909–13 guidelines, assessors first memorized the sweetness intensities and scores of reference samples (Table S1C). During testing, they evaluated HFCS samples using a 15-cm labeled line scale. Samples were gargled for 5 s, expectorated, and sweetness intensity was rated at predefined intervals (as above) via the Appsense V10.1.2 software. Testing was repeated in triplicate (3-h intervals between sessions).

2.9. Homology modeling of the sweet taste receptor

The amino acid sequences of the T1R2/T1R3 proteins were retrieved from the Uniprot (T1R2, UniProtKB: Q8TE23; T1R3, UniProtKB: Q7RTX0). Using Protein BLAST tool of the NCBI, a search was conducted in the Protein Data Bank (PDB) for crystal structures with high sequence similarity (Boratyn et al., 2012). A crystal structure, 7EPA(Du et al., 2021), exhibiting a sequence identity of 27 % was selected as the modeling template. The T1R2/T1R3 proteins were then subjected to homology modeling using the SWISS-MODEL (Swiss Institute of Bioinformatics, Lausanne, Switzerland), followed by molecular mechanics optimization of the protein models (Maier et al., 2015; Waterhouse et al., 2018). Finally, the PROCHECK program was utilized to assess the quality of the models.

2.10. Molecular docking

The constructed T1R2/T1R3 protein structure underwent molecular mechanics optimization, serving as the receptor for molecular docking. The structures of glucose, fructose, and menthol were built using the Build module of YASARA (YASARA Biosciences GmbH, Vienna, Austria), and each molecular structure was optimized using the GAFF force field, serving as ligands for molecular docking. AutoDock 4.2.6 and Autodock Tools 1.5.6(Scripps Research Institute, La Jolla, CA, USA) were used for receptor-ligand docking. The semi-flexible docking method was adopted for studying the binding mode of ligands molecules (glucose, fructose, menthol) and T1R2/T1R3. The docking box was designed to encompass the active site, with grid points set to 80 × 80 × 80 in the XYZ directions and a grid spacing of 0.375 Å. The number of docking runs was set to 100, with all other parameters remaining at their default values.

2.11. Molecular dynamic simulation

The molecular dynamic (MD) simulation was conducted using the Gromacs 2018.4 (Groningen University, Groningen, Netherlands) under constant temperature and pressure conditions with periodic boundary conditions. The Amber14SB all-atom force field and the TIP3P water model were employed. Throughout the MD simulation, bonds involving hydrogen atoms were constrained using the LINCS algorithm with an integration step size of 2 fs. Electrostatic interactions were computed using the Particle-mesh Ewald (PME) method, while non-bonded interactions were truncated at 10 Å and updated every 10 steps. The simulation temperature was maintained at 300 K using the V-rescale temperature coupling method, and the pressure was controlled at 1 bar using the Parrinello-Rahman method. Initially, both systems were subjected to energy minimization using the steepest descent method to eliminate close contacts between atoms. Subsequently, 100 ps of NVT and NPT equilibration simulations were performed at 310 K. Finally, a 100 ns MD simulation was conducted, with configurations saved every 10 ps. The visualization of simulation results was presented by Gromacs embedded program and VMD (University of Illinois at Urbana-Champaign, Urbana, IL, USA).

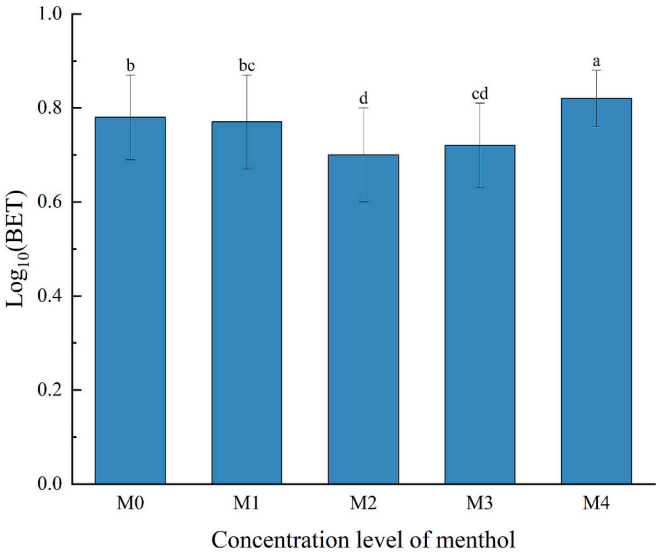

Fig. 1. The impact of menthol concentration levels on the sweetness recognition threshold of HFCS. M1, M2, M3, and M4 denote the concentrations of L-menthol in the samples, which are 0.004, 0.010, 0.030, and 0.060 g g/L. Different lowercase letters indicate statistically significant differences ($p < 0.05$).

2.12. Statistical analysis

Sensory data were collected and compiled using the APPsense V10.1.2. Microsoft Office Excel 2019 was employed for statistical analysis, including data aggregation, computation of means, and determination of standard deviations. Variance (ANOVA) analysis was conducted with IBM SPSS Statistics 27, while Origin 2022 was utilized for nonlinear curve fitting, principal component analysis, and graphical representation of the data.

3. Results and discussion

3.1. Sensory analysis of the enhancing effect of cooling stimulation on sweetness intensity

3.1.1. Enhancing effect of cooling stimulation on sweet taste sensitivity

Based on the calculation method described in Section 2.4, the sweetness group recognition thresholds of HFCS in pure water and solutions with varying menthol concentrations (0.004 g/L, 0.010 g/L, 0.030 g/L, 0.060 g/L) were determined as 5.98 g/L, 5.82 g/L, 5.02 g/L, 5.28 g/L, and 6.65 g/L, respectively. Referring to ISO 13301-2018, the dispersion of these thresholds was characterized by the standard deviation of their logarithmic values (See Fig. 1).

It is noteworthy that the 0.004 g/L menthol concentration selected in this study is the coolness threshold of menthol measured in our previous sensory evaluation. It is evident that threshold concentration of menthol had no significant ($p<0.05$) impact on the threshold of HFCS, consistent with the findings of Büchner et al. (2022).

Furthermore, it was observed that menthol, under 0.060 g/L, has the effect of lowering the sweet taste threshold of HFCS, suggesting that mild cooling stimulation primes taste receptor sensitivity. However, at 0.06 g/L, assessors qualitatively reported perceiving a bitter taste in addition to the cooling sensation-a known off-taste of menthol at elevated concentrations (Green & Schullery, 2003). The intense cooling sensation or bitter stimulation may divert attention away from taste, resulting in a decreased perception (Han et al., 2022). We focused on the impact of cool sensation on sweet taste perception, without conducting a quantitative assessment of bitterness. However, prior studies indicate that bitter stimulation not only enhances bitter signals in the brainstem

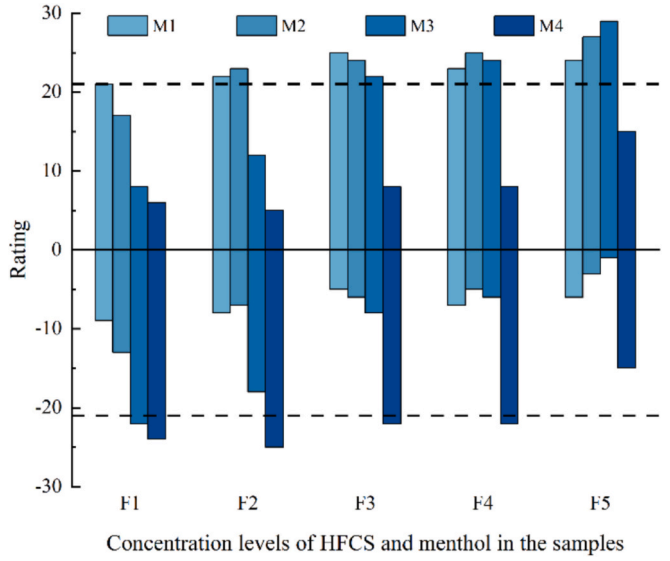

Fig. 2. Comparative analysis of sweetness scale results between the control and test samples. Each bar represents a test sample (e.g. the first bar represents test sample M1F1). The vertical axis indicates the number of assessors who preferred the test sample as sweeter. Positive values signify the number of assessors who chose the test sample, while negative values represent those who opted for the compared sample. Each sample was evaluated by a panel of 30 assessors. In this study, according to the ISO 5495:2005, a sample is deemed to have a significantly higher sweetness than the other if it is preferred by at least 21 assessors.

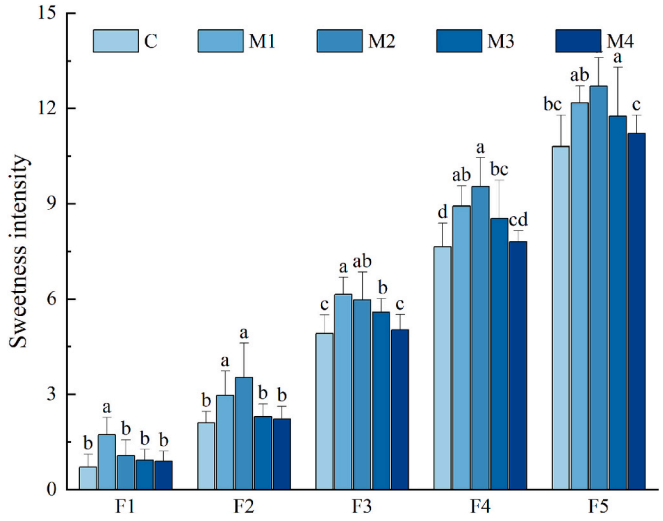

Fig. 3. The influence of varying intensities of menthol stimuli on the perception of sweetness.

but also triggers the brain cortex to suppress the desire for sweet substances, blunting the ability to perceive initial sweetness (Jin et al., 2021). This unintended bitterness may have confounded sweetness threshold measurements at higher menthol concentrations, highlighting a limitation of menthol as a cooling agent. Therefore, future studies exploring the effects of higher cooling intensities on the sweet taste threshold should consider using non-bitter cooling agents as alternatives to menthol, in order to eliminate the interference of bitterness.

3.1.2. *Concentration-response curves and reference scale of sweetness*

By pooling the results of the calibration for each descriptor and analyzing the maximum and minimum scale values, the panel established a comprehensive scaling range for each descriptor. The results showed that the sweetness descriptors could cover the common sweetness ranges found in beverages, with scale values ranging from 1.0 to 14.8 cm. Semantic overlaps among the descriptors were rectified through panel training and discussions. Arranged in ascending order of sweetness intensity, the scale ranges are as follows: slightly sweet (1.0–3.0 cm), a little sweet (3.0–6.9 cm), sweet (6.9–9.0 cm), relatively sweet (9.0–12.2 cm), and very sweet (12.2–14.8 cm) (See Fig. S1A). This serves as a scaling basis for subsequent research on sweetness perception.

The panel conducted three rounds of scoring for the sweetness intensity of HFCS reference samples with concentrations ranging from 6 to 68.3 g/L. The RSD values for the sweetness intensity reference sample scale results, whether evaluated by individual or panel, were within 0.20, indicating valid and stable data (See Table S2). A fitting analysis was conducted to correlate the concentrations of HFCS with their corresponding overall sweetness intensity values (See Fig. S1B). The results revealed a power function relationship between the concentration (C) and the overall sweetness intensity value (I), with a fitting equation of $I = 1.83C^{0.51}–3.72$ ($R^2 = 0.9962$), indicating an ideal fit. This demonstrates that there exists a power function correspondence between the psychological magnitude of the evaluator's perception of sweetness intensity and the physical magnitude of HFCS concentration, conforming to the general form of Stevens' psychophysical law (expressed as $S = k*I^n$). In essence, the assessor's response to sweetness intensity follows this law under the given concentration of HFCS. Finally, after discussion and consensus, the panel agreed on the overall sweetness rating values for the reference samples (See Fig. S1A), establishing a sweetness intensity reference system. Specifically, HFCS concentrations of 5.98 g/L (F1), 9.60 g/L (F2), 22.10 g/L (F3), 38.10 g/L (F4), and 57.20 g/L (F5) were chosen to represent the five sweetness intensity descriptors: threshold sweetness, slightly sweet, a little sweet, sweet, and relatively sweet.

3.1.3. *Assessing the sweetening enhancement of menthol through paired comparison tests and 15 cm linear scale*

This study compared and evaluated the sweetness perception of HFCS solutions with different cooling stimuli (M1-M4) against those without cooling stimuli. This preliminary exploration aimed to assess the impact of varying cooling intensities on the perception of sweetness.

Fig. 2 illustrates the influence of different cooling stimuli on the perception of HFCS sweetness. The following trends are observable: (a) The cooling stimulus of M1 significantly enhances the perception of sweetness for all concentrations of HFCS, ranging from F1 to F5. This suggests a synergistic effect between the cooling stimulus provided by M1 and the sweetness of the HFCS, resulting in a stronger perception of sweetness among the panelists. (b) The cooling stimulus of M2 produces a significant enhancement in the perception of sweetness for moderate to high concentrations of HFCS, specifically from F2 to F5. Compared to M1, M2 may exhibit less significant effects at lower concentrations but remains effective in enhancing sweetness perception at moderate to high concentrations. (c) The cooling stimulus of M3 is only effective in significantly sweetening HFCS at moderate to high concentrations (F3 to F5). This indicates that the cooling stimulus of M3 is more compatible with higher concentrations of the HFCS, producing a noticeable sweetening effect within these ranges. (d) Conversely, the cooling stimulus of M4 diminishes the perception of HFCS sweetness among panelists. To elucidate this, it is crucial to consider the role of multisensory information in perception. Research by Mishra and Gazzaley (2012) suggests that the distribution of attention when processing multisensory information significantly impacts perception. In the case of M4, intense cooling sensations or significant changes in cooling intensity from M3 to M4 may captivate the panelists' attention and increase their cognitive load, prompting them to focus more on the degree of cooling stimulation or the magnitude and variance of intensity changes, thereby diverting their attention away from sweetness and perceiving a decrease in

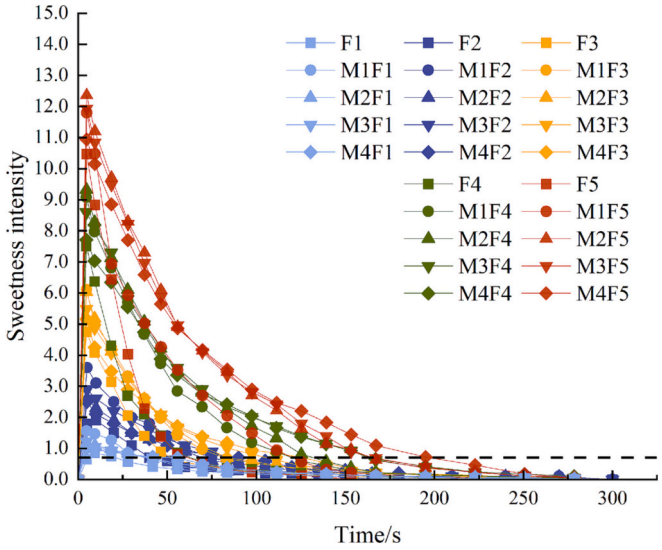

Fig. 4. The TI curves of cooling-sweetness systems.

sweetness(Floor et al., 2023). Alternatively, according to literature and panel feedback, the high concentration of menthol in M4 could have contributed to a bitter taste, which suppressed the perception of sweetness (Jin et al., 2021), resulting in a lower perception of sweetness compared to the compared sample.

The assessment of menthol's sweetening efficiency was conducted by quantifying the sweetness intensity using the 15 cm linear scale method. As depicted in Fig. 3, the results from this method exhibit a general concordance with those obtained through paired comparison testing.

However, discrepancies arise when it comes to the cooling stimulus of M4, the two methodologies yield divergent conclusions. The paired comparison test indicates that the cooling stimulus of M4 suppresses the perception of sweetness, whereas the linear scale method reveals no significant ($p<0.05$) difference in sweetness between the M4 cooling-sweetness system and a solution of HFCS with an equivalent concentration. Such differences may stem from the distinct focuses of the two evaluation methods. Quantitative estimation methods, such as the 15 cm linear scale approach, are particularly advantageous for assessing samples with pronounced differences. These techniques generate continuous data (e.g., scoring differentials) that enable panelists to articulate their sensory perceptions with greater nuance, thereby facilitating sophisticated analyses such as effect degree calculations. Difference testing methodologies amplify population preference signals through simplified binary decision-making and forced-choice paradigms. While this approach facilitates the detection of subtle yet consistent differences and mitigates systematic bias arising from inconsistent rating scales (e.g., lenient/strict scoring tendencies), it comes at the expense of quantitative information on the degree of difference. Synthesizing the results of both methodologies, it is evident that cooling-induced sweetness enhancement demonstrates marked stability in M1 and M2, with M3 exhibiting moderate efficacy. The impact of M4's cooling stimulus on sweet taste perception appears modulated by multiple covariates, including individual differences, experimental conditions, and analytical methods, necessitating further investigation in future studies.

Indeed, the static sweet intensity fails to account for the duration of stimulation and the intricate influence of cooling sensation within a complex sensory experience. Therefore, in evaluating how assessors discern this static "sweetness intensity" from the intricate temporal features and complex perceptual matrix, the impact of the temporal dimension must be taken into consideration.

3.1.4. Impact of cooling stimulation on dynamic perception characteristics of sweet taste

The TI curves for 25 cooling-sweet solutions were constructed (See Fig. 4) to investigate the dynamic influence of menthol on sweetness perception over time.

All samples exhibited a similar trend in sweetness, rapidly increasing to a peak within the first 5–10 s, followed by a gradual decline. The findings of Bian et al. (2023) indicate that sweetness perception is primarily determined from the initial 2–5 s of sensation, aligning with the observed T_{max} of 5 s in this study. Samples F1 and F2 reached sweetness

Table 1
The parameter information of TI curves of cooling-sweetness systems.

Sample	T^a_{ext}	$R^b_{decrease}$	I^c_{max}	T^d_{max}	$R^e_{increase}$	$T^f_{plateau}$	AUC^g
F1	31.85 ± 28.65b	−0.02 ± 0.01bc	0.93 ± 0.13c	12.00 ± 7.14a	0.10 ± 0.04c	11.11 ± 9.27a	57.85 ± 9.94b
M1F1	47.31 ± 17.01ab	−0.03 ± 0.02c	1.69 ± 0.32a	7.00 ± 4.58c	0.30 ± 0.10a	5.55 ± 3.90a	92.83 ± 11.97a
M2F1	48.50 ± 21.89ab	−0.02 ± 0.01ab	1.26 ± 0.24b	6.50 ± 2.29c	0.22 ± 0.08b	7.43 ± 3.97a	83.95 ± 11.27a
M3F1	51.58 ± 33.24ab	0.02 ± 0.01abc	1.23 ± 0.14b	5.50 ± 1.50c	0.24 ± 0.05ab	8.48 ± 7.75a	88.08 ± 12.31a
M4F1	62.00 ± 10.54a	−0.01 ± 0.00a	1.09 ± 0.14bc	9.00 ± 5.83ab	0.16 ± 0.07bc	9.00 ± 5.78a	88.65 ± 8.38a
F2	51.58 ± 29.79a	−0.04 ± 0.02a	2.05 ± 0.24c	8.00 ± 3.32a	0.30 ± 0.10c	6.84 ± 4.55b	84.38 ± 10.03b
M1F2	82.13 ± 49.73ab	−0.05 ± 0.04a	3.57 ± 0.29a	5.50 ± 1.50b	0.68 ± 0.13a	8.30 ± 5.71a	174.28 ± 21.98a
M2F2	82.85 ± 58.45ab	−0.04 ± 0.03a	2.63 ± 0.20b	5.50 ± 1.50b	0.50 ± 0.09b	8.53 ± 6.15a	141.28 ± 19.88a
M3F2	90.54 ± 47.86b	−0.04 ± 0.03a	2.93 ± 0.90b	5.50 ± 1.50b	0.56 ± 0.21ab	6.78 ± 3.67ab	171.55 ± 22.15a
M4F2	91.95 ± 69.77b	−0.03 ± 0.03a	2.45 ± 0.76bc	5.00 ± 0.00b	0.49 ± 0.15b	9.39 ± 9.00a	160.00 ± 28.76a
F3	62.24 ± 23.21b	−0.09 ± 0.04a	4.81 ± 0.61b	5.50 ± 1.50a	0.92 ± 0.21b	4.97 ± 3.19a	161.70 ± 16.38b
M1F3	101.27 ± 45.69ab	−0.09 ± 0.07a	6.22 ± 0.89a	5.50 ± 1.50a	1.20 ± 0.29a	5.79 ± 5.35a	272.75 ± 28.79a
M2F3	89.75 ± 39.65ab	−0.09 ± 0.07a	6.04 ± 0.75a	5.00 ± 0.00a	1.21 ± 0.15a	5.49 ± 2.85a	267.10 ± 27.85a
M3F3	103.44 ± 61.43ab	−0.08 ± 0.06a	5.51 ± 0.70ab	5.50 ± 1.50a	1.05 ± 0.22ab	7.66 ± 4.70a	288.13 ± 36.76a
M4F3	116.44 ± 59.53a	−0.06 ± 0.05a	5.15 ± 0.79b	5.00 ± 0.00a	1.03 ± 0.16ab	4.28 ± 2.34a	288.40 ± 39.27a
F4	69.32 ± 30.12b	−0.13 ± 0.07a	7.51 ± 0.99b	5.00 ± 0.00a	1.50 ± 0.20b	4.25 ± 1.19b	239.15 ± 22.21b
M1F4	113.51 ± 55.38ab	−0.12 ± 0.10a	9.08 ± 0.62a	5.00 ± 0.00a	1.82 ± 0.12a	7.72 ± 4.30ab	477.48 ± 51.05a
M2F4	128.88 ± 59.36ab	−0.10 ± 0.06a	9.33 ± 0.91a	5.00 ± 0.00a	1.87 ± 0.18a	6.98 ± 4.91ab	542.95 ± 56.94a
M3F4	145.65 ± 75.74a	−0.09 ± 0.07a	8.70 ± 1.21a	5.50 ± 1.50a	1.66 ± 0.38ab	11.07 ± 7.65a	594.83 ± 63.77a
M4F4	156.96 ± 77.28a	−0.06 ± 0.04a	7.71 ± 1.06b	5.00 ± 0.00a	1.54 ± 0.21b	9.97 ± 5.14a	565.78 ± 62.56a
F5	70.44 ± 25.71b	−0.18 ± 0.08a	10.48 ± 0.65c	5.00 ± 0.00a	2.10 ± 0.13b	4.86 ± 2.71b	294.86 ± 23.07b
M1F5	121.52 ± 54.26ab	−0.15 ± 0.12a	11.99 ± 1.01ab	5.50 ± 1.50a	2.29 ± 0.44ab	6.32 ± 4.09ab	646.45 ± 66.91a
M2F5	121.52 ± 54.27a	−0.12 ± 0.10a	12.37 ± 1.67a	5.00 ± 0.00a	2.47 ± 0.33a	9.07 ± 5.51ab	805.89 ± 74.50a
M3F5	121.52 ± 54.28a	−0.11 ± 0.08a	11.94 ± 1.24ab	5.00 ± 0.00a	2.39 ± 0.25ab	9.01 ± 5.02ab	802.35 ± 75.69a
M4F5	121.52 ± 54.29a	−0.09 ± 0.09a	10.97 ± 1.22bc	5.50 ± 1.50a	2.10 ± 0.44b	10.43 ± 5.32a	828.33 ± 78.87a

Note: [a] Sweetness extinction time. [b] Rate of intensity decrease following I_{max}. [c] Maximum sweetness intensity. [d] Time to reach I_{max}. [e] Rate of intensity increase prior to I_{max}. [f] Duration where sweetness intensity remains ≥90 % of I_{max}. [g] Area under the curve. Different lowercase letters within the same indicator denote statistically significant differences ($p < 0.05$).

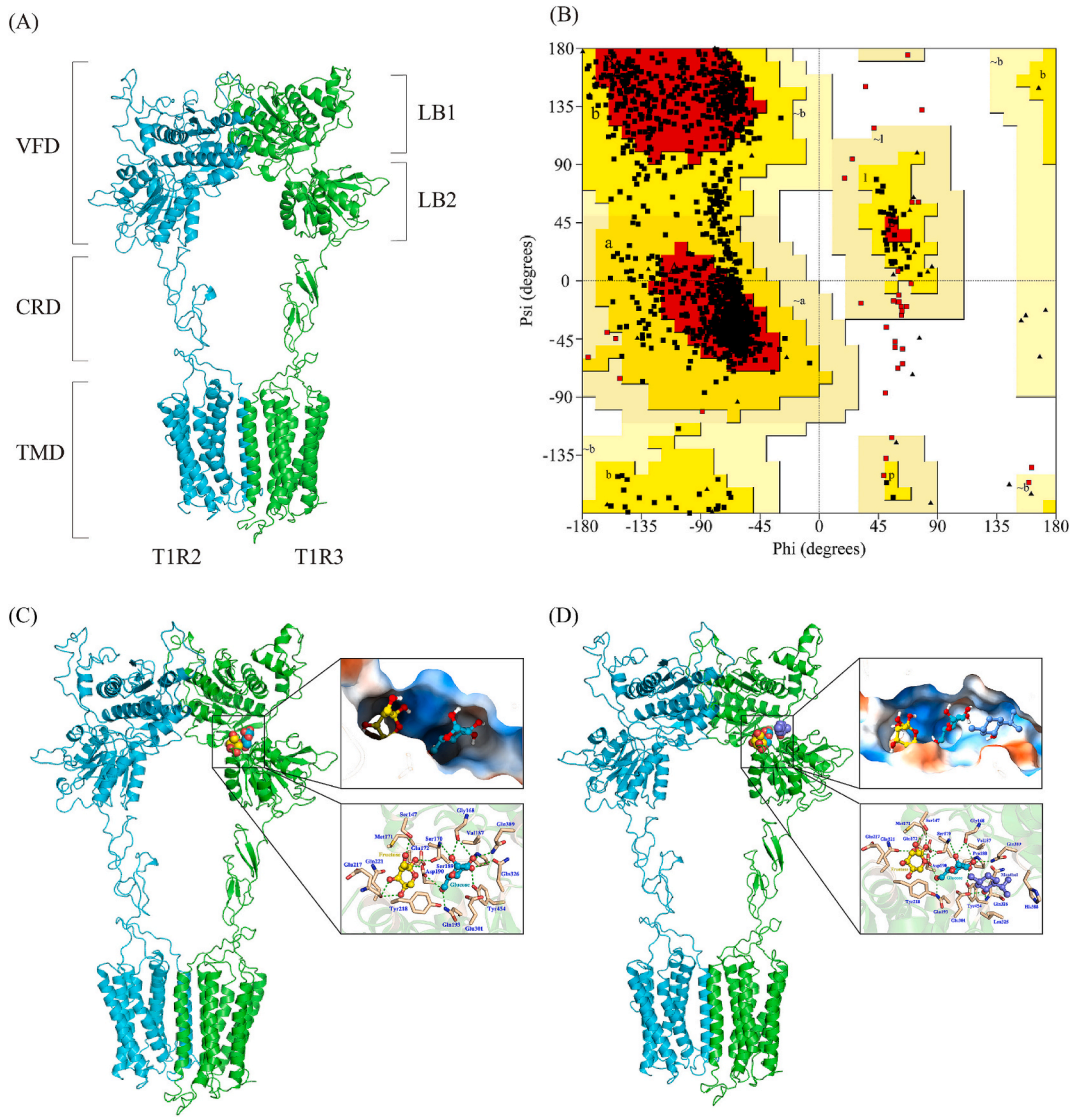

Fig. 5. The homology model structure of STR and molecular docking of ligand molecules with STR. (A) The homology model structure of STR. (B) Ramachandran plot of the model. (C) The molecular docking results and partial enlarged views of T1R2/T1R3-Glucose/Fructose system. (D) The molecular docking results and partial enlarged views of T1R2/T1R3-Glucose/Fructose/Menthol system. Ligand molecules: glucose (blue ball-and-stick), fructose (yellow ball-and-stick), and menthol (purple ball-and-stick). The upper images of partial enlarged views highlight the binding patterns of ligands on the hydrophilic(blue) and hydrophobic (orange) surfaces of the protein. The lower images depict the binding sites of ligands with STR amino acid residues (beige stick). (For interpretation of the references to colour in this figure legend, the reader is referred to the web version of this article.)

peak around the 10th second, likely due to their relatively lower sweetness levels, making it more difficult for assessors to detect and thus delaying the perception of maximum sweetness intensity. All samples maintained their peak intensity for approximately 5 s, followed by a gradual reduction. Furthermore, Fig. 4 highlights the concentrated sweetness of samples with the same concentration of HFCS, suggesting that the cooling sensation has a limited enhancing effect on the sweetness peak (I_{max}) and does not enhance the sweetness to a higher semantic description category. The data in Fig. 4 reveals that samples F4 and F5, without the addition of menthol, exhibit a shorter sweetness durations. This finding underscores the persistent feature of the cooling sensation induced by menthol, which contributes to extending the sweetness duration in the cooling-sweet hybrid system.

Based on the established reference system, when the assessors employed 0.84 cm as the criterion for sweetness evaluation, it signified the precise point at which the sweetness was perceptible or the threshold beyond which it became imperceptible in a descending evaluation. This critical value is denoted by a dashed black line in Fig. 4. To ensure experimental accuracy, during pre-experimental training and the formal evaluation, assessors were instructed to utilize scores below 0.84 cm to describe residual non-sweet sensations in the mouth as sweetness wanes. These sensations may encompass the gradual dominance of sourness, astringency sensation, or the cooling sensation induced by menthol. Consequently, in analysis of sweetness duration, we specifically refer to the time interval from the initial perception of sweetness to the moment when the assessor's assessment drops below 0.84 cm, thus gauging the persistence of sweetness.

To further evaluate the Temporal-Intensity characteristics of sweetness perception across varying degrees of cooling sensation, this study extracted seven characteristic parameters from the TI curves of 25 cooling sensation-sweetness systems (See Table 1).

As evident in Table 1, significant differences in five characteristic parameters (I_{max}, $T_{plateau}$, T_{ext}, $R_{increase}$ and AUC) were observed across varying cooling degrees for the same HFCS concentration. Notably, the similar distribution trends of samples based on I_{max} and $R_{increase}$, as well as $T_{plateau}$ and AUC, suggest a strong correlation between these pairs of

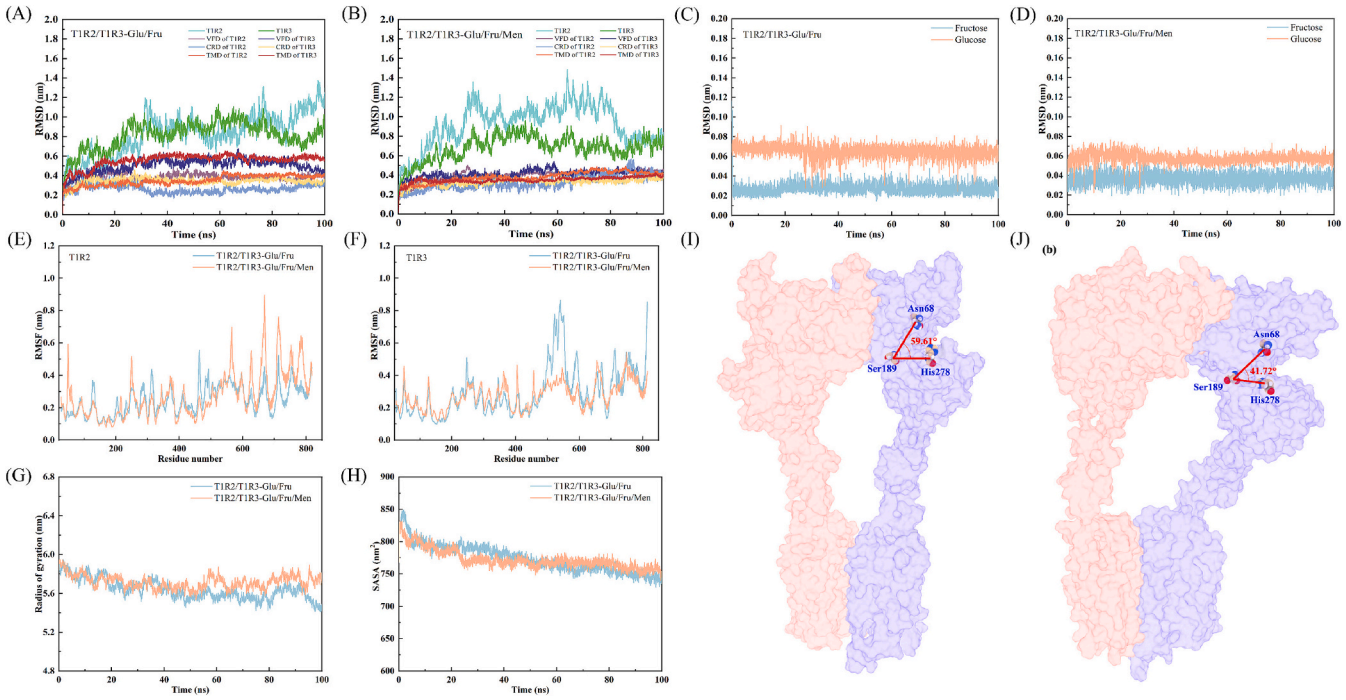

Fig. 6. Comparative analysis of stability in both systems. (A) RMSD of each domain in T1R2/T1R3-Glu/Fru; (B) RMSD of each domain in T1R2/T1R3-Glu/Fru/Men; (C) RMSD of glucose and fructose in T1R2/T1R3-Glu/Fru; (D) RMSD of glucose and fructose in T1R2/T1R3-Glu/Fru/Men; (E) RMSF of T1R2 in both systems; (F) RMSF of T1R3 in both systems; (G) Rg in both systems; (H) SASA in both systems; (I)Angular variations of the active site pocket in T1R2/T1R3-Glu/Fru; (J)Angular variations of the active site pocket in T1R2/T1R3-Glu/Fru/Men.

parameters. Specifically, the significant difference in I_{max} aligns with the findings in Fig. 3, indicating that M1 to M3 exhibit a certain sweetness-enhancing effect, while M4 lacks such an effect. Additionally, T_{ext} displayed a significant difference ($p < 0.05$) between the groups with and without menthol. These results suggest that the overall sweetness perception by evaluators is primarily governed by two parameters: I_{max} and T_{ext}. Consequently, in practical applications, one can initially determine the initial concentration of HFCS based on the target sweetness range, and subsequently, enhance sweetness intensity and prolong sweetness duration through appropriate menthol addition, ultimately achieving sweetness enhancement or reduction in HFCS addition.

To mitigate potential psychological biases in the assessment process, this study employed the Single-Attribute Time-Intensity (SATI) method for a sustained and focused evaluation of the sweetness attribute. Ideally, to precisely identify the potential impact of cooling sensation on sweetness perception, the Multi-Attribute Time-Intensity (MATI) method should be utilized, concurrently assessing both cooling and sweetness attributes in one sample (Kuesten et al., 2013). This approach would not only eliminate inherent differences between samples but also reduce the time and cost of evaluation. However, given the current limitations of cooling sensation evaluation methods and the heightened perceptual acuity required for assessing this chemesthesis, the study opts for the SATI method as the primary tool for evaluating sweetness attributes, pending the refinement of cooling sensation evaluation techniques.

3.2. Molecular mechanism of menthol enhancing sweet taste perception

3.2.1. Homology modeling of STR and molecular docking of ligand molecules with STR

This study successfully constructed a T1R2/T1R3 sweet receptor protein model by SWISS-MODEL program, and its accuracy was rigorously evaluated through the PROCHECK program. As illustrated in Ramachandran plot (Fig. 5B), a remarkable 97.5 % of amino acid residues in this model reside in the favored region, while 99.40 % of their dihedral angles fall within acceptable ranges, adhering to stereochemical energy principles, thus affirming the reliability of this model's structure. Consequently, the protein model is deemed reasonable and can serve as a template for subsequent investigations.

This study employs the comprehensive T1R2/T1R3 structure (Fig. 5A) for molecular simulations. The human STR belongs to the Class C GPCRs, consisting of a heterodimer protein formed by T1R2 and T1R3 subunits. As evident in Fig. 5A, it comprises three distinct parts: an extracellular Venus flytrap domain (VFD) with a sizable central cavity and a leaf-like structure, a transmembrane domain (TMD) region composed of seven helical structures, and a cysteine-rich domain (CRD) that bridges the two. The VFD serves as the primary binding site for molecules such as glucose, fructose, and sucrose, critical for the STR to perceive sweet signals (DuBois, 2016). Therefore, a thorough analysis of the interactions between this domain and ligands could contribute significantly to elucidating the molecular mechanism underlying menthol's enhancement of sweet perception.

In molecular simulation, menthol, glucose, and fructose were docked as ligands with T1R2/T1R3, contrasting with a system devoid of menthol (glucose-fructose-T1R2/T1R3 complex). Docking scores indicate: glucose-T1R2 at −3.66 kcal/mol, glucose-T1R3 at −3.84 kcal/mol; fructose-T1R2 at −3.06 kcal/mol, and fructose-T1R3 at −3.84 kcal/mol, all docking within the VFD of T1R2 or T1R3. Similar to findings by Kashani-Amin et al. (2019) glucose and fructose molecules bind within the active pocket of VFD of T1R3, with varying selectivity for different ligands and STR conformations. Absolutely, based on binding affinity, both ligands preferentially bind to the T1R3 subunit. Fig. 5C-D depict the binding conformation and sites of menthol-glucose-fructose-T1R2/T1R3 complex. Clearly, glucose, fructose, and menthol primarily bind within the hydrophilic cavity of T1R3's VFD, consistent with Chéron et al. (2017) exhibiting extensive hydrogen bonding interactions with surrounding amino acid residues.

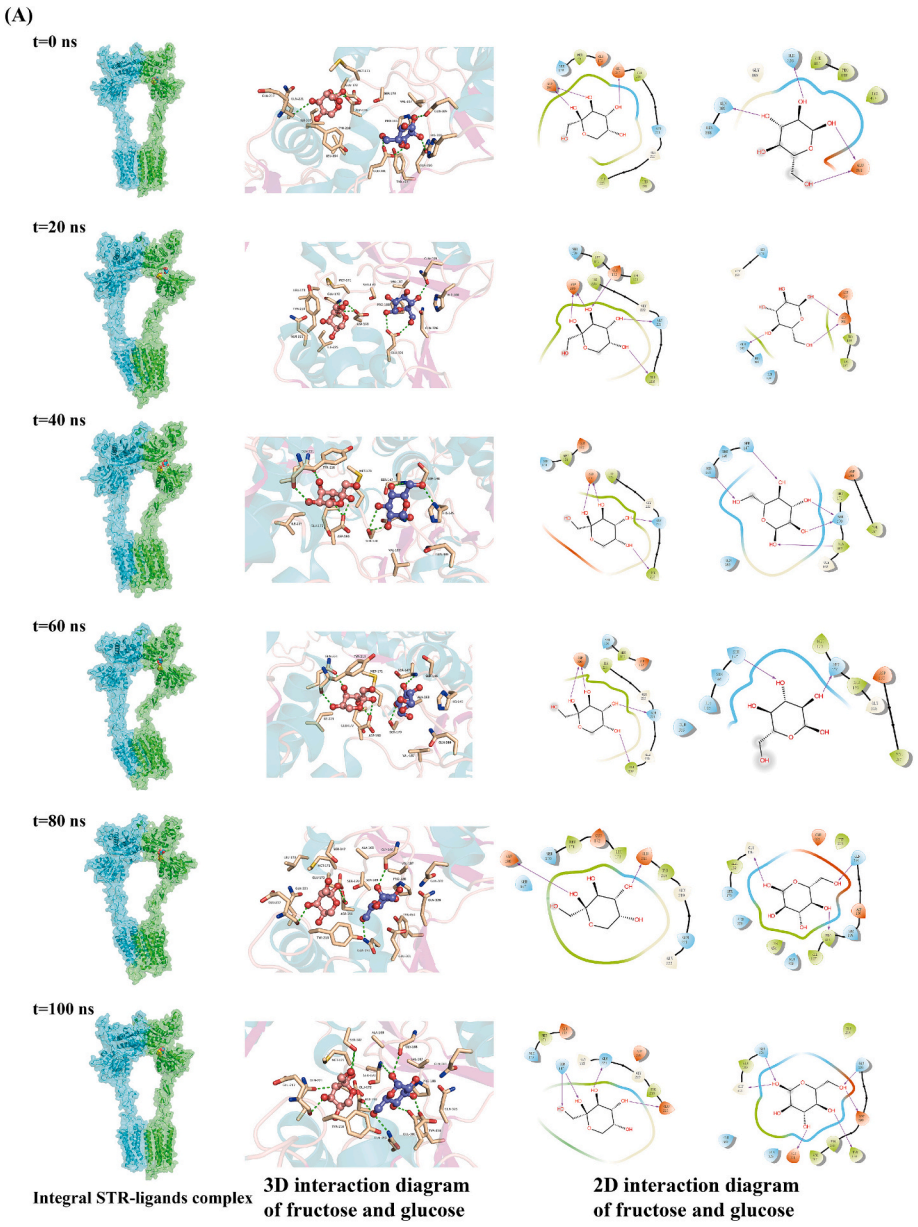

Fig. 7. The binding sites and conformations of the both systems during simulation.

3.2.2. Impact of menthol on the structural stability of T1R2/T1R3-glucose/fructose complex

To further elucidate the molecular recognition mechanisms and docking stability between three ligands and proteins, this study conducted MD simulations on the binding of menthol, glucose, and fructose with STR.

The root mean square deviation (RMSD), which reflects the sum of atomic deviations from the target conformation, is a crucial indicator for assessing system stability. In comparing Fig. 6A-B, during the simulation, it was observed that the RMSD fluctuations of the T1R3 subunit, when bound to menthol, were significantly reduced compared to the T1R2 subunit. This diminution in fluctuation is postulated to be a result of menthol binding, which restricts the mobility of the T1R3 subunit. A further analysis of each domain within T1R2 and T1R3 revealed that menthol had a relatively minor impact on the conformational changes of each domain in T1R2, whereas it significantly influenced the conformations of VFD and TMD of T1R3. Specifically, menthol binding reduced the RMSD of T1R3's VFD from fluctuating around 0.56 nm to a more stable range around 0.41 nm, and similarly, the RMSD of T1R3's TMD decreased from 0.58 to 0.34. The RMSD analysis also served to evaluate the stability of the ligands relative to STR during the simulation. As depicted in Fig. 6C-D, the RMSD values of glucose and fructose remained consistently low and stable, indicating a robust binding between the ligands and STR. Notably, the addition of menthol did not lead to significant conformational changes or dissociation of glucose and fructose from STR.

The root mean square fluctuation (RMSF) serves as a metric for quantifying the flexibility of amino acid residues in proteins. As illustrated in Fig. 6E-F, the amino acid flexibility distribution in T1R2/T1R3 proteins reveals that the binding of menthol and T1R3 significantly enhances the RMSF in the Res560-Res830 region of T1R2 while diminishing it in the Res500-Res600 region of T1R3. This indicates that the binding of menthol to the VFD of T1R3 augments the atomic fluctuations in the CRD of T1R2 while reducing those in the terminal region of the CRD of T1R3 and the first two transmembrane helices of its TMD. The CRD and TMD of T1R3 not only serve as active binding sites for

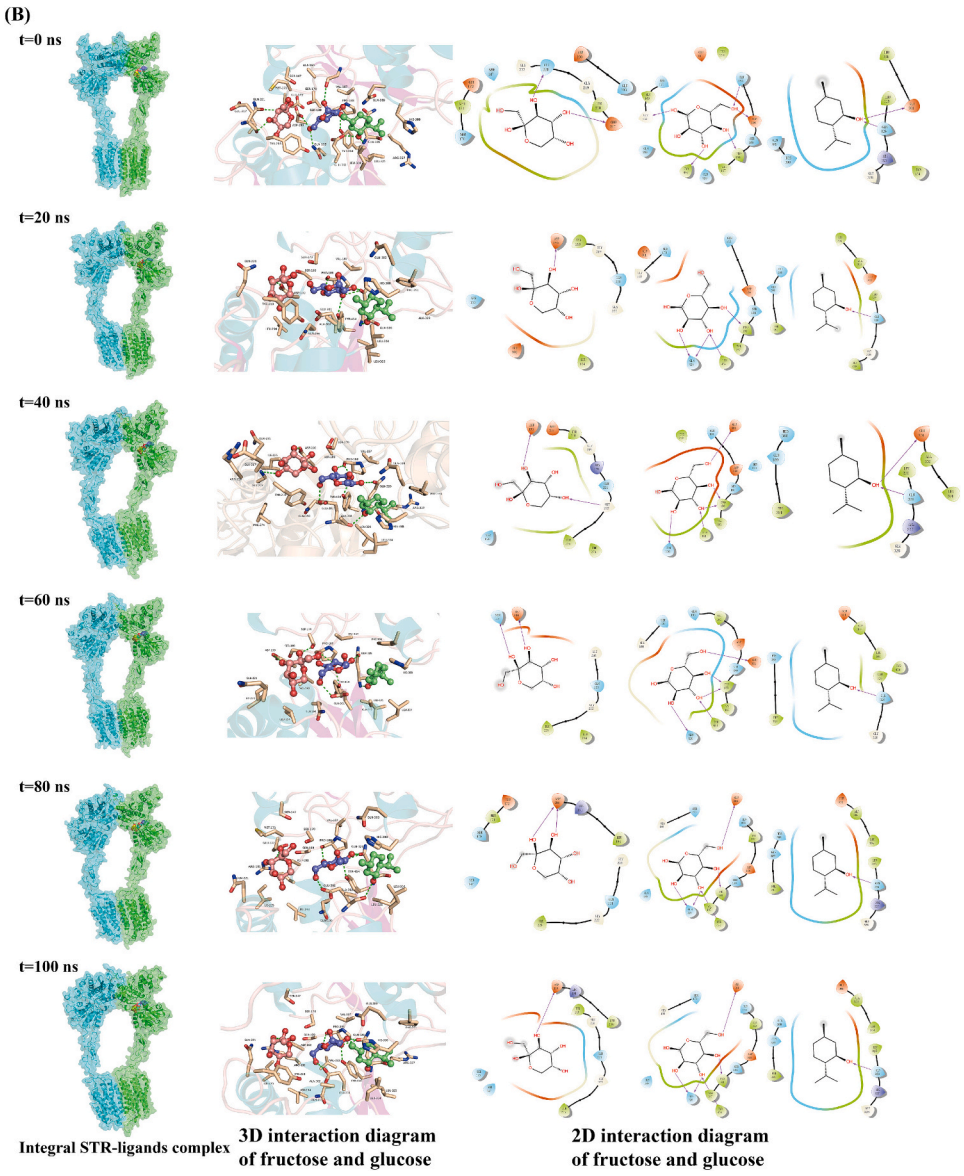

Fig. 7. (*continued*).

high-intensity sweeteners but also participate in the transduction of sweet taste signals (Jang et al., 2021; Kim et al., 2017). Therefore, it is plausible that menthol exerts a sweet-enhancing effect by influencing the transduction of these sweet taste signals.

The Radius of Gyration (Rg) serves to quantify the extent of conformational changes, where a larger Rg indicates a more expanded structure. As observed in Fig. 6G, both systems exhibit a relatively stable level of expansion. Notably, the Rg of T1R2/T1R3-Glu/Fru/Men slightly surpasses T1R2/T1R3-Glu/Fru after 60 ns, indicating a marginal swelling induced by menthol.

The solvent-accessible surface area (SASA), reflecting the interface between protein and solvent, serves as a proxy for conformational changes in proteins. Fig. 6H reveal a gradual yet indistinctive decline in SASA for both systems. Post 60 ns, the average SASA values for T1R2/T1R3-Glu/Fru and T1R2/T1R3-Glu/Fru/Men are 753.95 $\pm$ 7.72 nm^2 and 763.24 $\pm$ 7.21 nm^2, respectively. In the later stages of the simulation, the slight elevation in protein expansion and SASA observed in T1R2/T1R3-Glu/Fru/Men suggests that, while the overall protein structure remains largely unaltered, the addition of menthol potentially enhances the accessibility of previously concealed or inaccessible active sites for interactions with solvents (such as water molecules) or other glucose and fructose molecules.

An in-depth analysis of the angular variations of three amino acids (Asn68, Ser189, and His278) situated near the active site of T1R3 in two distinct systems has been conducted to elucidate the effect of Menthol on the interaction between LB1 and LB2. As illustrated in Fig. 6I-J, a noticeable reduction in the angular range of the active site is observed in the T1R2/T1R3-Glu/Fru/Men system, suggesting a propensity towards closure of the T1R3 active site after 100 ns of MD simulation. This configuration favors stable binding of glucose and fructose molecules within the active site, minimizing their escape from the pocket. Zhang et al. (2024) demonstrated that the sweet signal of natural sweet substances (taking sucrose as an example) is generally transmitted through the cyclic adenosine monophosphate (cAMP) pathway. When sweet substances bind to the sweet taste receptors T1R2/T1R3, they activate the G α subunit and adenylate cyclase to produce cAMP. cAMP activates protein kinase A, causing potassium ion channel phosphorylation and inhibiting potassium ion efflux, thereby triggering membrane polarization and neurotransmitter release, generating electrical signals to stimulate peripheral nerves, and transmitting them to the taste center of the brain through the chordal nervous system, ultimately perceiving sweetness. Sweetness enhancers, on the other hand, do not activate STR

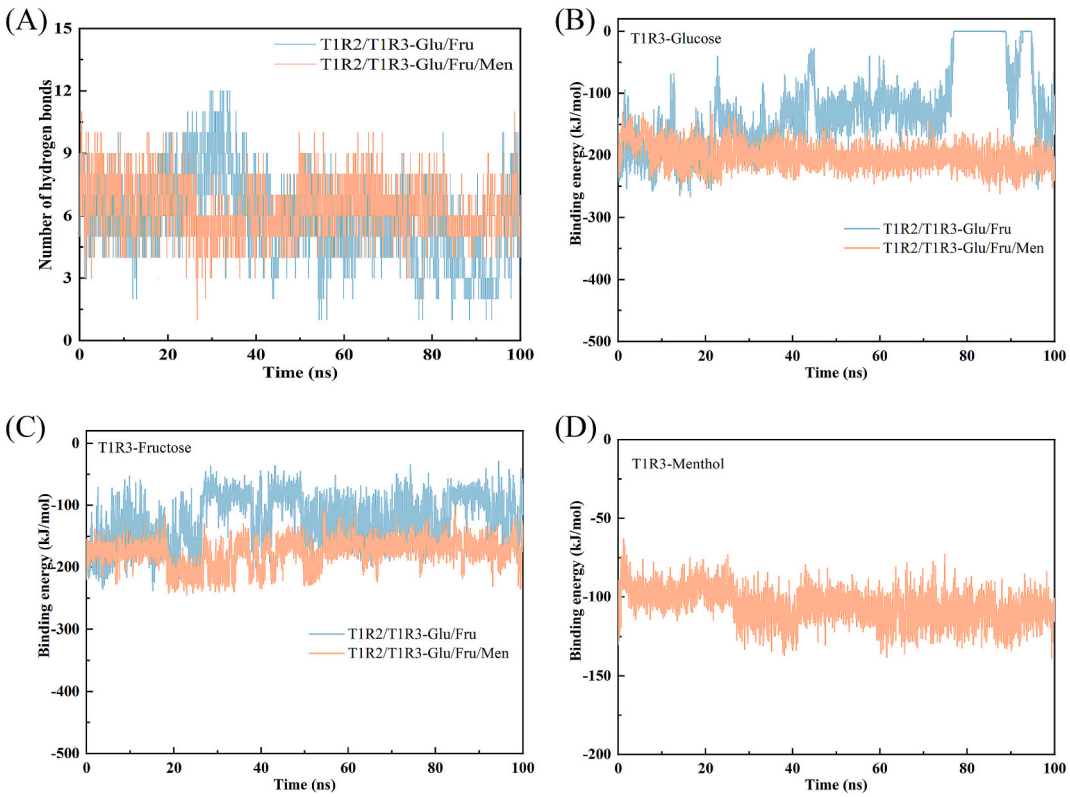

Fig. 8. Interaction of ligands with T1R2/T1R3 protein in both systems during simulation. (A) The total number of hydrogen bonds between glucose and fructose with STR; (B) Binding energy between glucose and T1R3;(C) Binding energy between fructose and T1R3; (D) Binding energy between menthol and T1R3.

but rather stabilize the closed state of the VFD domain by binding to it in both T1R2 and T1R3 subunits, thereby enhancing the affinity between sugar molecules and STR, ultimately intensifying sweet taste perception (Ahmad & Dalziel, 2020; Monique et al., 2018). In their exploration of the binding patterns between STR and low-molecular-weight sweeteners, Masuda and his colleagues discovered that the interaction between LB1 and LB2 is pivotal for the recognition of all sweeteners. The interactions at the pocket entrance formed by LB1 and LB2 facilitate the formation of the STR's closed structure, which is essential for its activation (Masuda et al., 2012). Further research conducted by Zhang et al. (2010) and Yamada et al. (2019) has revealed that sweetness enhancers enhance sweetness perception by strengthening the hydrophobic interactions between the two lobes of the VFD, LB1 and LB2, and reducing the free energy required for its closure, thereby stabilizing the closed conformation.

3.2.3. Effect of menthol on the interaction between sweet taste molecules and T1R2/T1R3 protein

This study further examines the interplay between the ligands and the T1R2/T1R3 protein. Fig. 7 depicts the changes in the interaction between the ligands and the T1R2/T1R3 protein at 0 ns, 20 ns, 40 ns, 60 ns, 80 ns, and 100 ns during the simulation. This figure reveals that the ligands stably bind to STR through hydrogen bonding and hydrophobic interactions, exhibiting no tendency to escape from STR.

Interaction of ligand molecules with T1R2/T1R3 Protein in T1R2/T1R3-Glu/Fru (A) and T1R2/T1R3-Glu/Fru/Men (B) during Simulation.

Upon analyzing the amino acid sites involved in docking, within the T1R2/T1R3-Glu/Fru system, glucose exhibits high binding frequencies with amino acid residues such as Gly168, Ser170, Asp190, Gln193, Glu301, and Gln389, stabilized by hydrogen bonds. Similarly, fructose also displays high binding frequencies with residues like Ser147, Ser170, Glu217, and Gln221, forming hydrogen bonds. However, in the T1R2/T1R3-Glu/Fru/Men system, the pattern of hydrogen bonding between glucose, fructose, and specific amino acid residues undergoes alterations, with menthol also forming stable hydrogen bonds with residues like Glu301 and Gln326. The active cavity constituted by these amino acid residues represents the active binding site. Currently, there is limited research reporting on the active sites of natural small molecular sugars (such as glucose, fructose, and sucrose) binding to the VFD of T1R3. Kashani-Amin et al. (2019) have suggested that the VFD active site of T1R3 for α-D-glucooligosaccharides are primarily constituted by amino acid residues like E148, H281, S306, L308, L331, L385, N386, H387, H388, Q389, and F391. Notably, the Ser147 residue, which fructose docks with, has been proven crucial for the sensitivity of sugar molecules in activating STR (Dubovski et al., 2023).

Upon analyzing the binding patterns of ligands and STR in the two systems from a conformational perspective, an analysis of the hydrogen bond counts and binding energy changes in both systems was conducted (Fig. 8). Fig. 8A illustrates that the hydrogen bond interactions between glucose and fructose with T1R3 in the T1R2/T1R3-Glu/Fru/Men system, with the addition of menthol, are more stable compared to the T1R2/T1R3-Glu/Fru system. From the observation of the binding sites of glucose, fructose, and menthol in Fig. 7, it is evident that the inclusion of menthol occupies a portion of the active cavity, shifting glucose and fructose towards the left, thereby altering the position of hydrogen bonding and consequently influencing their interactions with the STR. Zhang et al. (2010)posit that in the combined effect of sucrose/sucralose and enhancers, the enhancer occupies partial sites within the receptor's active pocket, thereby achieving a binding mode akin to that of stevioside.

Fig. 8B-D highlights the changes in binding energies between the ligands and STR in both systems. In the T1R2/T1R3-Glu/Fru/Men system, the binding energies of glucose and fructose with STR exhibit a relatively stable trend, averaging at -208.96 ± 15.59 kJ/mol and -167.39 ± 15.91 kJ/mol, respectively. In contrast, the T1R2/T1R3-Glu/Fru system, devoid of menthol, displays significant fluctuations in the

binding energies of glucose and fructose with the STR, averaging at −77.65 ± 66.25 kJ/mol and − 117.79 ± 32.44 kJ/mol, respectively. This comparison underscores the substantial enhancement in the binding of glucose and fructose with the STR induced by the inclusion of menthol. Fig. 8D further demonstrates that the binding energy of menthol itself with the STR is also relatively stable, averaging at −110.25 ± 9.13 kJ/mol. This indicates that menthol molecules can stably bind to the active site of the T1R3, potentially providing a robust foundation for its enhancing effect on glucose and fructose molecules. Zhang et al. (2010) propose that the sweetening mechanism of taste enhancers follows a "docking-locking" two-step mechanism. The sweetener Initially binds to the hinge region, inducing the closure of the VFT domain (docking). Subsequently, the enhancer binds near the opening, further stabilizing the closed conformation (locking). The entropy loss incurred during the closure process is compensated by the binding of the enhancer, thereby ensuring binding stability.

4. Conclusion

In this study, the cooling agent, menthol, exhibits a notable capability to potentiate the sensory perception of sweetness in HFCS. Specifically, menthol lowers the sweetness detection threshold, elevates maximum perceived intensity, and prolongs sweetness duration. Further molecular modeling reveals the potential mechanism by which menthol enhances sweetness: menthol molecules stably bind near the binding sites of glucose and fructose with the STR. This binding facilitates two critical actions: (1) By altering glucose/fructose conformations, menthol strengthens hydrogen bonding between these ligands and the receptor's VFD. (2) Menthol enhances hydrophobic interactions near the ligand-binding pocket, stabilizing the closed VFD conformation required for receptor activation. Additionally, menthol may strengthen sweet taste perception by affecting the transduction of sweet signals. These combined effects likely amplify downstream signal transduction, linking molecular interactions to perceptual outcomes, necessitating further validation and revelation through biological experiments and electroencephalography techniques in future studies.

Ethical statement

The content of the sensory evaluation experiment has been informed consent of the candidates and has been carried out in accordance with The Code of Ethics of the World Medical Association (Declaration of Helsinki). Research protocols of sensory evaluation by panelists were approved by the Shanghai Institute of Technology Ethics Committee.

CRediT authorship contribution statement

Haiyan Yu: Writing – review & editing, Writing – original draft, Resources, Methodology, Formal analysis, Conceptualization. **Ting Ao:** Writing – original draft, Software, Methodology, Investigation, Formal analysis. **Haifang Mao:** Supervision, Resources. **Jibo Liu:** Supervision, Resources. **Chen Chen:** Supervision, Resources, Formal analysis. **Huaixiang Tian:** Writing – review & editing, Project administration.

Declaration of competing interest

The authors declare that they have no known competing financial interests or personal relationships that could have appeared to influence the work reported in this paper.

Acknowledgments

The authors sincerely thank the panelists for their support in sensory evaluation.

Appendix A. Supplementary data

Supplementary data to this article can be found online at https://doi.org/10.1016/j.fochx.2025.102337.

Data availability

Data will be made available on request.

References

Ahmad, R., & Dalziel, J. E. (2020). G protein-coupled receptors in taste physiology and pharmacology. *Frontiers in Pharmacology, 11*, Article 587664. https://doi.org/10.3389/fphar.2020.587664

Ai, Y., & Han, P. (2022). Neurocognitive mechanisms of odor-induced taste enhancement: A systematic review. *International Journal of Gastronomy and Food Science, 28*, Article 100535. https://doi.org/10.1016/j.ijgfs.2022.100535

Bian, J. M., Xia, Y. X., Han, R. J., Wang, C. Y., He, J., & Zhong, F. (2023). How to determine Iso-sweet concentrations for various sweeteners: Insights from consumers and trained panels. *Food Quality and Preference, 107*, Article 104824. https://doi.org/10.1016/j.foodqual.2023.104824

Biswas, D., & Szocs, C. (2019). The smell of healthy choices: Cross-modal sensory compensation effects of ambient scent on food purchases. *Journal of Marketing Research, 56*(1), 123–141. https://doi.org/10.1177/0022243718820585

Boratyn, G. M., Schäffer, A. A., Agarwala, R., Altschul, S. F., Lipman, D. J., & Madden, T. L. (2012). Domain enhanced lookup time accelerated BLAST. *Biology Direct, 7*(1), Article 12. https://doi.org/10.1186/1745-6150-7-12

Büchner, K., Haagen, J., Sastrosubroto, A., Kerpes, R., Freiherr, J., & Becker, T. (2022). Trigeminal stimulus menthol masks bitter off-flavor of artificial sweetener Acesulfame-K. *Foods, 11*(18), Article 2734. https://doi.org/10.3390/foods11182734

Chen, L., Wu, W., Zhang, N., Bak, K. H., Zhang, Y., & Fu, Y. (2022). Sugar reduction in beverages: Current trends and new perspectives from sensory and health viewpoints. *Food Research International, 162*, Article 112076. https://doi.org/10.1016/j.foodres.2022.112076

Chéron, J. B., Golebiowski, J., Antonczak, S., & Fiorucci, S. (2017). The anatomy of mammalian sweet taste receptors. *Proteins: Structure, Function, and Bioinformatics, 85*(2), 332–341. https://doi.org/10.1002/prot.25228

Deliza, R., Lima, M. F., & Ares, G. (2021). Rethinking sugar reduction in processed foods. *Current Opinion in Food Science, 40*, 58–66. https://doi.org/10.1016/j.cofs.2021.01.010

Du, J., Wang, D. J., Fan, H. C., Xu, C. J., Tai, L. H., Lin, S. L., … Zhao, Q. (2021). Structures of human mGlu2 and mGlu7 homo- and heterodimers. *Nature, 594*(7864), 589–593. https://doi.org/10.1038/s41586-021-03641-w

DuBois, G. E. (2016). Molecular mechanism of sweetness sensation. *Physiology & Behavior, 164*(Part B), 453–463. https://doi.org/10.1016/j.physbeh.2016.03.015

Dubovski, N., Galeczki, Y. B. S., Malach, E., & Niv, M. Y. (2023). Sensitivity of human sweet taste receptor subunits T1R2 and T1R3 to activation by glucose enantiomers. *Chemical Senses, 48*, Article bjad005. https://doi.org/10.1093/chemse/bjad005

Floor, V. M., Henk, V. S., & Lotte, F. V. D. (2023). The effect of cognitive load on preference and intensity processing of sweet taste in the brain. *Appetite, 188*, Article 106630. https://doi.org/10.1016/j.appet.2023.106630

Green, B. G., & Schullery, M. T. (2003). Stimulation of bitterness by capsaicin and menthol: Differences between lingual areas innervated by the glossopharyngeal and Chorda tympani nerves. *Chemical Senses, 28*(1), 45–55. https://doi.org/10.1093/chemse/28.1.45

Han, P. F., Müller, L., & Hummel, T. (2022). Peri-threshold trigeminal stimulation with capsaicin increases taste sensitivity in humans. *Chemosensory Perception, 15*(1), 1–7. https://doi.org/10.1007/s12078-021-09285-4

ISO 13301. (2018). *Sensory analysis-Methodology-General guidance for measuring odour, flavour and taste detection thresholds by a three-alternative forced-choice (3-AFC) procedure*. Geneva: International Organization for Standardization.

Jang, J., Kim, S.-K., Guthrie, B., Goddard, W. A., & III.. (2021). Synergic effects in the activation of the sweet receptor GPCR heterodimer for various sweeteners predicted using molecular Metadynamics simulations. *Journal of Agricultural and Food Chemistry, 69*(41), 12250–12261. https://doi.org/10.1021/acs.jafc.1c03779

Jin, H., Fishman, Z. H., Ye, M. Y., Wang, L., & Zuker, C. S. (2021). Top-down control of sweet and bitter taste in the mammalian brain. *Cell, 184*(1), 257–271. https://doi.org/10.1016/j.cell.2020.12.014

Johnson, S., Tian, M., Sheldon, G., & Dowd, E. (2018). Trigeminal receptor study of high-intensity cooling agents. *Journal of Agricultural and Food Chemistry, 66*(10), 2319–2323. https://doi.org/10.1021/acs.jafc.6b04838

Kashani-Amin, E., Sakhteman, A., Larijani, B., & Ebrahim-Habibi, A. (2019). Presence of carbohydrate binding modules in extracellular region of class C G-protein coupled receptors (C GPCR): An *in silico* investigation on sweet taste receptor. *Journal of Biosciences, 44*(6), Article 138. https://doi.org/10.1007/s12038-019-9944-9

Kim, S. K., Chen, Y., Abrol, R., Goddard, W. A., & Guthrie, B. (2017). Activation mechanism of the G protein-coupled sweet receptor heterodimer with sweeteners and allosteric agonists. *Proceedings of the National Academy of Sciences of the United States of America, 114*(10), 2568–2573. https://doi.org/10.1073/pnas.1700001114

Kuesten, C., Bi, J., & Feng, Y. (2013). Exploring taffy product consumption experiences using a multi-attribute time–intensity (MATI) method. *Food Quality and Preference, 30*(2), 260–273. https://doi.org/10.1016/j.foodqual.2013.06.007

Maier, J. A., Martinez, C., Kasavajhala, K., Wickstrom, L., Hauser, K. E., & Simmerling, C. (2015). ff14SB: Improving the accuracy of protein side chain and backbone parameters from ff99SB. *Journal of Chemical Theory and Computation, 11*(8), 3696–3713. https://doi.org/10.1021/acs.jctc.5b00255

Maluly, H. D. B., Johnston, C., Giglio, N. D., Schreiner, L. L., Roberts, A., & Abegaz, E. G. (2020). Low- and no- calorie sweeteners (LNCS): Critical evaluation of their safety and health risks. *Food Science and Technology, 40*(1), 1–10. https://doi.org/10.1590/fst.36818

Masuda, K., Koizumi, A., Nakajima, K.-I., Tanaka, T., Abe, K., Misaka, T., & Ishiguro, M. (2012). Characterization of the modes of binding between human sweet taste receptor and low-molecular-weight sweet compounds. *PLoS One, 7*(4), Article e35380. https://doi.org/10.1371/journal.pone.0035380

McDonald, S. T., Bolliet, D. A., & Hayes, J. E. (2016). Types of chemesthesis II: Cooling. In *Chemesthesis-chemical touch in food and eating* (pp. 106–133). John wiley & sons: New Jersey, USA.

Miele, N. A., Cabisidan, E. K., Plaza, A. G., Masi, P., Cavella, S., & Di Monaco, R. (2017). Carbohydrate sweetener reduction in beverages through the use of high potency sweeteners: Trends and new perspectives from a sensory point of view. *Trends in Food Science and Technology, 64*, 87–93. https://doi.org/10.1016/j.tifs.2017.04.010

Mishra, J., & Gazzaley, A. (2012). Attention distributed across sensory modalities enhances perceptual performance. *The Journal of Neuroscience, 32*(35), 12294–12302. https://doi.org/10.1523/JNEUROSCI.0867-12.2012

Monique, C. B., Thiago, D., & Juliano, D. D. L. (2018). Sweeteners and sweet taste enhancers in the food industry. *Food Science and Technology, 38*(2), 181–187. https://doi.org/10.1590/fst.31117

da Portela, C. D., Viencz, T., dos Santos, K. L. B., Lima, T., & de Benassi, M. D. (2024). Added sugar in coffee beverages: A study with a sample of Brazilian consumers of sweetened and unsweetened coffee. *Journal of Sensory Studies, 39*(2), Article e12911. https://doi.org/10.1111/joss.12911

Rocha, R. A. R., Ribeiro, M. N., Silva, G. A., Rocha, L. C. R., Pinheiro, A. C. M., Nunes, C. A., & Carneiro, J. D. S. (2020). Temporal profile of flavor enhancers MAG, MSG, GMP, and IMP, and their ability to enhance salty taste, in different reductions of sodium chloride. *Journal of Food Science, 85*(5), 1565–1575. https://doi.org/10.1111/1750-3841.15121

Sun, X. X., Zhong, K., Zhang, D., Shi, B. L., Wang, H. Y., Shi, J. Y., … Zhao, L. (2023). Saltiness enhancement by "m'a l'a" umami flavor in NaCl model aqueous and oil-added systems. *Food Research International, 173*, Article 113277. https://doi.org/10.1016/j.foodres.2023.113277

Vidal, L., Antúnez, L., Ares, G., Cuffia, F., Lee, P. Y., Le Blond, M., & Jaeger, S. R. (2019). Sensory product characterisations based on check-all-that-apply questions: Further insights on how the static (CATA) and dynamic (TCATA) approaches perform. *Food Research International, 125*, Article 108510. https://doi.org/10.1016/j.foodres.2019.108510

Wang, Y., Zhong, K., Shi, B. L., Wang, H. Y., Liu, L. Y., Zhang, L. L., … Gao, H. Y. (2022). Cross-modal effect of capsaicin and pepper oleoresin on the enhancement of saltiness perception in a NaCl model solution. *Food Quality and Preference, 98*, Article 104542. https://doi.org/10.1016/j.foodqual.2022.104542

Waterhouse, A., Bertoni, M., Bienert, S., Studer, G., Tauriello, G., Gumienny, R., … Schwede, T. (2018). SWISS-MODEL: Homology modelling of protein structures and complexes. *Nucleic Acids Research, 46*(W1), W296–W303. https://doi.org/10.1093/nar/gky427

WHO. (2015). *Guideline: Sugars intake for adults and children*. Geneva: World Health Organization.

Xu, L. Z., Han, Y. L., Chen, X. Y., Aierken, A., Wen, H., Zheng, W. J., … Yang, F. (2020). Molecular mechanisms underlying menthol binding and activation of TRPM8 ion channel. *Nature Communications, 11*(1), Article 3790. https://doi.org/10.1038/s41467-020-17582-x

Yamada, K., Nakazawa, M., Matsumoto, K., Tagami, U., Hirokawa, T., Homma, K., … Kitajima, S. (2019). Unnatural tripeptides as potent positive allosteric modulators of T1R2/T1R3. *ACS Medicinal Chemistry Letters, 10*(5), 800–805. https://doi.org/10.1021/acsmedchemlett.9b00051

Yuan, Y. Y., Yiasmin, M. N., Tristanto, N. A., Chen, Y. J., Liu, Y. X., Guan, S. Y., … Hua, X. (2024). Computational simulations on the taste mechanism of steviol glycosides based on their interactions with receptor proteins. *International Journal of Biological Macromolecules, 255*, Article 128110. https://doi.org/10.1016/j.ijbiomac.2023.128110

Zhai, T., Wang, J., Li, L., & Si, W. (2024). Taxing sugar-sweetened beverages in China: By volume or sugar content? A consumer welfare approach. *Journal of Integrative Agriculture, 23*(12), 4237–4249. https://doi.org/10.1016/j.jia.2024.10.006

Zhang, F., Klebansky, B., Fine, R. M., Liu, H., Xu, H., Servant, G., … Li, X. (2010). Molecular mechanism of the sweet taste enhancers. *Proceedings of the National Academy of Sciences, 107*(10), 4752–4757. https://doi.org/10.1073/pnas.0911660107

Zhang, L. L., Wang, H. Y., Shi, B. L., Zhi, R. C., Xie, N., Zhao, L., & Chen, X. H. (2016). Establishment of reference scale for and dynamic temporal change of cooling intensity. *Food Science, 37*(03), 38–42. https://doi.org/10.7506/spkx1002-6630-201603008

Zhang, Y. X., Li, X., Hu, J. X., Bi, J. F., & Liu, X. (2024). Research Progress in taste characteristics of fruits and fruit products and methods for their regulation. *Food Science, 45*(14), 299–311. https://doi.org/10.7506/spkx1002-6630-20230926-242

Zhao, L., Zhang, L. L., Shi, B. L., Wang, H. Y., & Zhi, R. C. (2015). A study on the establishment of labeled line scale for quantitative sensory evaluation of pungent intensity of Zanthoxyluml bungeanum. *Journal of Chinese Institute of Food Science and Technology, 15*(10), 211–216. https://doi.org/10.16429/j.1009-7848.2015.10.029

Zhao, S., Ma, S., Zhang, Y., Gao, M., Luo, Z., & Cai, S. (2024). Combining molecular docking and molecular dynamics simulation to discover four novel umami peptides from tuna skeletal myosin with sensory evaluation validation. *Food Chemistry, 433*, Article 137331. https://doi.org/10.1016/j.foodchem.2023.137331

Zhu, Z., Zhang, W., Li, Z., Zhao, W., Liu, C., Zhu, B., … Yang, Q. (2024). Rethinking sweetener discovering: Multiparameter modeling of molecular docking results between the T1R2–T1R3 receptor and compounds with different tastes. *Journal of Agricultural and Food Chemistry, 72*(13), 7336–7343. https://doi.org/10.1021/acs.jafc.4c00407